The effects of intrinsic noise on the behaviour of bistable cell regulatory systems under quasi-steady state conditions

Roberto de la Cruz[1,2], **Pilar Guerrero**[3], **Fabian Spill**[4,5], and **Tomás Alarcón**[1,2]

[1]Centre de Recerca Matemàtica. Edifici C, Campus de Bellaterra, 08193 Bellaterra (Barcelona), Spain

[2]Departament de Matemàtiques, Universitat Autònoma de Barcelona, 08193 Bellaterra (Barcelona), Spain

[3]Department of Mathematics, University College London, Gower Street, London WC1E 6BT, United Kingdom

[4]Department of Biomedical Engineering, Boston University, 44 Cummington Street, Boston, Massachusetts 02215, USA

[5]Department of Mechanical Engineering, Massachusetts Institute of Technology, 77 Massachusetts Avenue, Cambridge, Massachusetts 02139, USA

Abstract

We analyse the effect of intrinsic fluctuations on the properties of bistable stochastic systems with time scale separation operating under quasi-steady state conditions. We first formulate a stochastic generalisation of the quasi-steady state approximation based on the semi-classical approximation of the partial differential equation for the generating function associated with the chemical master equation. Such approximation proceeds by optimising an action functional whose associated set of Euler-Lagrange (Hamilton) equations provides the most likely fluctuation path. We show that, under appropriate conditions granting time scale separation, the Hamiltonian can be re-scaled so that the set of Hamilton equations splits up into slow and fast variables, whereby the quasi-steady state approximation can be applied. We analyse two particular examples of systems whose mean-field limit has been shown to exhibit bi-stability: an enzyme-catalysed system of two mutually inhibitory proteins and a gene regulatory circuit with self-activation. Our theory establishes that the number of molecules of the conserved species is order parameters whose variation regulates bistable behaviour in the associated systems beyond the predictions of the mean-field theory. This prediction is fully confirmed by direct numerical simulations using the stochastic simulation algorithm. This result allows us to propose strategies whereby, by varying the number of molecules of the three conserved chemical species, cell properties associated to bistable behaviour (phenotype, cell-cycle status, etc.) can be controlled.

I Introduction

The networks of interacting genes and proteins that are responsible for regulation, signalling and response, and which, ultimately, orchestrate cell function, are under the effect of noise. [1–5] This randomness materialises in the form of fluctuations of the number of molecules of the species involved, subsequently leading to fluctuations in their activity. Besides external

perturbations, biochemical reactions can be intrinsically noisy, especially when the number of molecules is very low.

Far from necessarily being a mere disturbance, fluctuations are an essential component of the dynamics of cellular regulatory systems which, in many instances, are exploited to improve cell function.[6,7] For example, randomness has been shown to enhance the ability of cells to adapt and increase their fitness in random or variable environments.[8–10] Random noise also serves the purpose of assisting cell populations to sustain phenotypic variation by enabling cells to explore the phase space.[3–5,7,11,12]

One of the mechanisms that allows noise-induced phenotypic variability relays on multi-stability.[13,14] The basis of this mechanism was first proposed by Kauffman,[15] who associated phenotypes or differentiated states to the stable attractors of the dynamical systems associated to gene and protein interaction networks. In the presence of noise, the corresponding phase space generates an epigenetic landscape, where cells exposed to the same environment and signalling cues coexist in different cellular phenotypes.[16]

Multi-stability is also an essential element in the control of cell response and function via signalling pathways.[17] In particular, bi-stability as a means to generate reliable switching behaviour is widely utilised in numerous pathways such as the apoptosis,[18] cell survival,[19] differentiation,[20] and cell-cycle progression[21,22] pathways. For example, bi-stability is used to regulate such critical cell functions such as the transition from quiescence to proliferation through bistable behaviour associated with the Rb-E2F switch within the regulatory machinery of the mammalian cell-cycle.[23–28]

A common theme which appears when trying to model cell regulatory systems is separation of time scales, i.e., the presence of multiple processes evolving on widely diverse time scales. When noise is ignored and systems are treated in terms of deterministic mean-field descriptions, such separation of time scales and the associated slow-fast dynamics are often exploited for several forms of model reduction, of which one of the most common is the so-called quasi-steady state approximation (QSSA).[29] This approximation is ubiquitously used whenever regulatory processes involve enzyme catalysis, which is a central regulation mechanism in cell function.[17] In this paper, we investigate the effects of intrinsic noise on the bi-stability of two particular systems, namely, an enzyme-catalysed system of mutual inhibition and a gene regulatory circuit with self-activation. The mean-field limit of both these systems has been shown to exhibit bi-stability.[22,30] The aim of this paper is to analyse how noise alters the mean-field behaviour associated to these systems when they operate under quasi-steady state conditions.

We note that this work does not concern the subject of noise-induced bifurcations.[31] Such phenomenon has been studied in many situations, including biological systems. An example which is closely related to the systems we analyse here is the so-called enzymatic futile cycles. Samoilov *et al.*[32] have shown that noise associated to the number of enzymes induces bistability. In the absence of this source of noise, i.e., in the mean-field limit, the system does not exhibit bistable behaviour. The treatment of these phenomena would require

to go to higher orders in the Wentzel–Kramers–Brillouin (WKB) expansion,[57] which we do not explore here.

The issue of separation of time scales in stochastic models of enzyme catalysis has been addressed using a number of different approaches. Several such analyses have been carried out in which the QSSA is directly applied to the master equation by setting the fast reactions in partial equilibrium (i.e., the probability distribution corresponding to the fast variables remains unchanged), and letting the rest of the system to evolve according to a reduced stochastic dynamic.[33,34] Other approaches have been proposed such as the QSSA to the exact Fokker-Planck equation that can be derived from the Poisson representation of the chemical master equation (CME).[35] Approaches based on enumeration techniques have also been formulated.[36] Furthermore, Thomas *et al.*[37] have recently formulated a rigorous method to eliminate fast stochastic variables in monostable systems using projector operators within the linear noise approximation.[37] Methods for model reduction based on perturbation analysis have been developed in Refs. 38 and 39. Additionally, driven by the need of more efficient numerical methods, there has been much activity regarding the development of numerical methods for stochastic systems with multiple time scales.[40–42] Several of these methods are variations of the stochastic simulation algorithm[33,43–47] or the τ-leap method[48] where the existence of fast and slow variables is exploited to enhance their performance with respect to the standard algorithms. Another family of such numerical methods is that of the so-called hybrid methods, where classical deterministic rate equations or stochastic Langevin equations for the fast variables are combined with the classical stochastic simulation algorithm for the slow variables.[49,50] Other related methods were studied in Refs. 51–53.

Here, we advance the formalism developed in Ref. 38, in which a method based on the semi-classical approximation of the chemical master equation allows to evaluate the effects of intrinsic random noise under quasi-steady conditions. In our analysis of the Michaelis-Menten model of enzyme catalysis in Ref. 38, we showed that the semi-classical quasi-steady state approximation (SCQSSA) reveals that the velocity of the enzymatic reaction is modified with respect to the mean-field estimate by a quantity which is proportional to the total number of molecules of the (conserved) enzyme. In this paper, we extend this formalism to show that, associated to each conserved molecular species, the associated (constant) number of molecules is a bifurcation parameter which can drive the system into bi-stability beyond the predictions of the mean-field theory. We then proceed to test our theoretical results by means of direct numerical simulation of the chemical master equation using the stochastic simulation algorithm.[54] We should note that the Hamiltonian formalism derived from the semi-classical approximation is formulated on a continuum of particles, which requires the number of particles to be large enough. This must hold true for all the species in our model, both fast and slow. Since this separation between fast and slow species is based on their relative abundance, one must be careful that the scaling assumptions are consistent, particularly in the case of the model of self-activating gene regulatory circuit where the number of binding sites is typically small. This assumption, however, has been used in previous studies.[55] Also we show that our simulation results of the full stochastic processes agree with our analysis and, therefore, our re-scaled equations are able to predict the behaviour of the system. We note that the mean-field limit, which is conventionally

obtained by ignoring noise in the limit of large particle numbers, is obtained by setting the momenta in our phase-space formalism to 1.

The approximation we develop in this paper falls within the general framework of the optimal fluctuation path theory.[56] This framework is a particular case of the large deviation theory which allows us to study rare events (i.e., events whose frequency is exponentially small with system size). Within these frameworks, we will show that, upon carrying out the QSSA, the only source of noise in the system is associated to the random initial conditions of the species whose numbers are conserved. We therefore predict that a population of cells, each having a random number of conserved molecules, will have a bimodal distribution.

This paper is organised as follows. Section II is devoted to a detailed exposition of the semi-classical quasi-steady state approximation for stochastic systems. In Sections III and IV, we apply this formalism to analyse the behaviour of a bistable enzyme-catalysed system and a gene regulatory circuit of auto-activation, respectively. We will show that our semi-classical quasi-steady state theory allows us to study the effect of intrinsic noise on the behaviour of these systems beyond the predictions of their mean-field descriptions. We also verify our theoretical predictions by means of direct stochastic simulations. Finally, in Section V, we summarise our results and discuss their relevance.

II Semi-Classical Quasi-Steady State Approximation

Our aim in this paper is to formulate a stochastic generalisation of the quasi-steady state approximation for enzyme-catalysed reactions and simple circuits of gene regulation and use such approximation to determine if the presence of noise has effects on the behaviour of the system beyond the predictions of the corresponding mean-field models. Specifically, we analyse stochastic systems for which the mean-field models predict bi-stability and investigate how such behaviour is affected by stochastic effects. Our analysis is carried out in the context of Markovian models of the corresponding reaction mechanisms formulated in terms of the so-called CME.[57] Two examples of such stochastic systems, a bistable enzyme-catalysed system and a gene regulatory circuit of auto-activation, are formulated and analysed in detail in Sections III and IV, respectively. Following Ref. 38, we formulate the QSS approximation for the asymptotic solution of the CME obtained by means of large deviations/WKB approximations.[58–60] The CME is given as

$$\frac{\partial P(X,t)}{\partial t} = \sum_i \big(W_i(X - r_i)P(X - r_i, t) - W_i(X)P(X,t)\big), \quad (1)$$

where $W_i(X)$ is the transition rate corresponding to reaction channel i and r_i is a vector whose entries denote the change in the number of molecules of each molecular species when reaction channel i fires up, i.e., $P(X(t + \Delta t) = X(t) + r_i | X(t)) = W_i(X)\,\Delta t$.

An alternative way to analyse the dynamics of continuous-time Markov processes on a discrete space of states is to derive an equation for the generating function, $G(p_1, \ldots, p_n, t)$, of the corresponding probabilistic density,

$$G(p_1, \ldots, p_n, t) = \sum_x p_1^{X_1} p_2^{X_2} \cdots p_n^{X_n} P(X_1, \ldots, X_n, t), \quad (2)$$

where $P(X_1, \ldots, X_n, t)$ is the solution of master equation (1). $G(p_1, \ldots, p_n, t)$ satisfies a partial differential equation (PDE) which can be derived from the master equation. This PDE is the basic element of the so-called momentum representation of the master equation.[51,53,61–63]

Although closed, analytic solutions are rarely available, the PDE for the generating function admits a perturbative solution, which is commonly obtained by means of the WKB method. [63] More specifically, the (linear) PDE that governs the evolution of the generating function can be written as

$$\frac{\partial G}{\partial t} = H_k(p_1, \ldots, p_n, \partial_{p_1}, \ldots, \partial_{p_n}) G(p_1, \ldots, p_n, t), \quad (3)$$

where the operator H_k is determined by the reaction rates of master equation (1). Furthermore, the solution to this equation must satisfy the normalisation condition $G(p_1 = 1, \ldots, p_n = 1, t) = 1$ for all t. This PDE, or, equivalently, the operator H, is obtained by multiplying both sides of master equation (1) by $\prod_{i=1}^{n} p_i^{X_i}$ and summing up over all the possible values $(X_1, \ldots, X_n)$.

From the mathematical point of view, Eq. (3) is a Schrödinger-like equation and, therefore, there is a plethora of methods at our disposal in order to analyse it. In particular, when the fluctuations are (assumed to be) small, it is common to resort to WKB methods.[58,59,64] This approach is based on the WKB-like Ansatz that $G(p_1, \ldots, p_n, t) = e^{-S(p_1, \ldots, p_n, t)}$. By substituting this Ansatz in Eq. (3), we obtain the following Hamilton-Jacobi equation for the function $S(p_1, \ldots, p_n, t)$:

$$\frac{\partial S}{\partial t} = -H_k\left(p_1, \ldots, p_n, \frac{\partial S}{\partial p_1}, \ldots, \frac{\partial S}{\partial p_n}\right). \quad (4)$$

Instead of directly tackling the explicit solution of Eq. (4), we will use the so-called semi-classical approximation. We use the Feynman path-integral representation which yields a solution to Eq. (3) of the type[58,62,65–68]

$$G(p_1, \ldots p_n, t) = \int_0^t e^{-S(p_1, \ldots, p_n, Q_1, \ldots, Q_n)} \mathfrak{D}Q(s)\mathfrak{D}p(s), \quad (5)$$

where $\mathscr{D}Q(s)\mathscr{D}p(s)$ indicates integration over the space of all possible trajectories and $S(p_1, \ldots, p_n, Q_1, \ldots, Q_n)$ is given by[58]

$$S(p_1, \ldots, p_n, Q_1, \ldots, Q_n) = -\int_0^t \left(H_k(p_1, \ldots, p_n, Q_1, \ldots, Q_n) + \sum_{i=1}^n Q_i(s)\dot{p}_i(s) \right) ds \quad (6)$$
$$+ \sum_{i=1}^n S_{0,i}(p_i, Q_i),$$

where the position operators in the momentum representation have been defined as $Q_i \equiv \ _{p_i}$ with the commutation relation $[Q_i, p_j] = S_{0,i}\delta_{i,j}$. $S_{0,i}(p_i, Q_i)$ corresponds to the action associated with the generating function of the probability distribution function of the initial value of each variable, $X_i(t = 0)$, which is assumed to be independent random variables.

The so-called semi-classical approximation consists of approximating the path integral in Eq. (5) by

$$G(p_1, \ldots, p_n, t) = e^{-S(p_1, \ldots, p_n, t)}, \quad (7)$$

where $p_1(t), \ldots, p_n(t)$ are now the solutions of the Hamilton equations, i.e., the orbits which maximise the action S,

$$\frac{dp_i}{dt} = -\frac{\partial H_k}{\partial Q_i}, \quad (8)$$

$$\frac{dQ_i}{dt} = \frac{\partial H_k}{\partial p_i}, \quad (9)$$

where the pair (Q_i, p_i) is the generalised coordinates corresponding to chemical species $i = 1, \ldots, n$. These equations are (formally) solved with boundary conditions67 $Q_i(0) = x_i(0)$, $p_i(t) = p_i$, where $x_i(0)$ is the initial number of molecules of species i.

Eqs. (8) and (9) are the starting point for the formulation of the SCQSSA.38 In order to proceed further, we assume, as per the Briggs-Haldane treatment of the Michaelis-Menten model for enzyme kinetics,26,69 that the species involved in the system under scrutiny are divided into two groups according to their characteristic scales. More specifically, we have a subset of chemical species whose numbers, X_i, scale as

$$X_i = Sx_i, \quad (10)$$

where $x_i = O(1)$, whilst the remaining species are such that their numbers, X_j, scale as

$$X_j = Ex_j, \quad (11)$$

where $x_j = O(1)$. Key to our approach is the fact that S and E must be such that

$$\epsilon = \frac{E}{S} \ll 1. \quad (12)$$

We further assume that the generalised coordinates, Q_i, scale in the same fashion as the corresponding variable X_i, i.e.,

$$Q_i = Sq_i, \quad (13)$$

where $q_i = O(1)$. We refer to the variables belonging to this subset as *slow variables*. Similarly,

$$Q_j = Eq_j, \quad (14)$$

where $q_j = O(1)$, which are referred to as *fast variables*. Moreover, we assume that the moment coordinates, p_i, are all independent of S and E and therefore remain invariant under rescaling.

Under this scaling for the generalised coordinates, we define the following scale transformation for the Hamiltonian in Eq. (6):

$$H_k(p_1, \dots, p_n, Q_1, \dots, Q_n) = k_J S^k E^l H_\kappa(p_1, \dots, p_n, q_1, \dots, q_n), \quad (15)$$

where J identifies the reaction with the largest order among all the reactions that compose the dynamics and k_J is the corresponding rate constant. For example, in the case of the bistable enzyme-catalysed system whose reactions or elementary events and the corresponding transition rates are given in Table I, $J = 1$, as this reaction is order 3 whereas all the others are order 0, 1, or 2. In the case of the self-activating gene regulatory circuit, Table IV, $J = 3$, since this reaction is order 3 whereas the remaining ones are order 1 at most. The exponents k and l correspond to the number of slow and fast variables involved in the transition rate W_J, respectively.

The last step is to rescale the time variable so that a dimensionless variable, τ, is defined such that

$$\tau = k_J S^{k-1} E^l t. \quad (16)$$

It is now a trivial exercise to check that, upon rescaling, Eqs. (8) and (9) read

$$\frac{dp_i}{d\tau} = -\frac{\partial H_\kappa}{\partial q_i}, \quad (17)$$

$$\frac{dq_i}{d\tau} = \frac{\partial H_\kappa}{\partial p_i} \quad (18)$$

for the slow variables. By contrast, rescaling of the Hamilton equations corresponding to the subset of fast variables leads to

$$\epsilon\frac{dp_j}{d\tau} = -\frac{\partial H_\kappa}{\partial q_j}, \quad (19)$$

$$\epsilon\frac{dq_j}{d\tau} = \frac{\partial H_\kappa}{\partial p_j}, \quad (20)$$

where ϵ is defined in Eq. (12). The QSS approximation consists on assuming that $\epsilon\frac{dp_j}{d\tau} \simeq 0$ and $\epsilon\frac{dq_j}{d\tau} \simeq 0$ in Eqs. (19) and (20),

$$-\frac{\partial H_\kappa}{\partial q_j} = 0, \quad (21)$$

$$\frac{\partial H_\kappa}{\partial p_j} = 0, \quad (22)$$

resulting in a differential-algebraic system of equations which provides us with the SCQSSA.

III   Bistable Enzyme-Catalysed Systems

As a prototype of a bistable enzyme-catalysed system, we analyse a stochastic system proposed in Refs. 38 and 70, whose mean-field limit has been shown to correspond to a bistable system which is a part of a model for the G_1/S transition of the eukaryote cell cycle proposed in Ref. 22. Tyson and Novak22 have formulated a (deterministic) model of the cell cycle such that the core of the system regulating the G_1/S transition is a system of two mutually repressing proteins (Cdh1 and CycB). This system of mutual repression gives rise

to a bistable system where one of the stable steady states is identified with the G_1 phase whereas the other corresponds to a state where the cell is ready to go through the other three phases of the cell-cycle, known as S, G_2, and M. This central module, which is the one we focus on, is acted upon by a complex regulatory network which monitors if conditions are met for the cell to undergo this transition and accounts for its accurate timing. Presently, we ignore this network and focus on the central bistable system. It is shown in Ref. 22 that the mean field version of the model exhibits bistable behaviour as a function of a bifurcation parameter m, i.e., the mass of the cell. For very small values of m, the system is locked into a high (low) Cdh1(CycB)-level stable fixed point (i.e., into the G_1 phase). For very large values m, the system has only one stable steady state corresponding to a low (high) Cdh1(CycB)-level fixed point. For intermediate values of m, the system exhibits bistability, i.e., both of these stable fixed points coexist with an unstable saddle point. In this section, we focus on how noise alters the behaviour of the mean-field dynamics.

The transition rates corresponding to the different reactions involved in the stochastic model associated to the enzyme-regulated kinetics shown in Fig. 1 are given in Table I. This kinetics corresponds to the enzyme regulated activation and inhibition of Cdh1 (an inhibitor of cell-cycle progression). Cdh1 inactivation is further (up)regulated by the presence of CycB, an activator of cell-cycle progression. CycB is synthesised and degraded at basal rates and is further degraded in the presence of active Cdh1 (see Fig. 1). Therefore, the resulting dynamics leads to a system with mutual inhibition which produces bistable behaviour. It is important to note that the associated reaction kinetics exhibits three conservation laws (see Table I): $X_3 + X_5 = e_0$, $X_4 + X_6 = e_0$, and $X_1 + X_2 + X_5 + X_6 = s_0$. The first two of these conservation laws are associated to the conservation of the number of Cdh1-inhibiting and Cdh1-activating enzymes, respectively, whilst the latter expresses the conservation of the total number of Cdh1 molecules. The quantities e_0 and s_0 are the (conserved) number of enzymes and Cdh1, respectively. Note that, as per the methodology developed in Section II, we assume that $s_0 = O(S)$ and $e_0 = O(E)$.

The corresponding stochastic Hamiltonian, H_k, which is derived by applying the methodology of Section II to the master equation associated to the chemical kinetics described in Table I, can be split into three parts,

$$H_k(p_1, \ldots, p_7, Q_1, \ldots, Q_7) = H_A + H_I + H_B, \quad (23)$$

where H_I is the Hamiltonian corresponding to the CycB-regulated enzymatic inactivation of Cdh1 (reactions 1 to 3 in Table I),

$$\begin{aligned} H_1(p, Q) = {} & k_4(p_6 - p_2 p_4)Q_2 Q_4 + k_5(p_2 p_4 - p_6)Q_6 \\ & + k_6(p_1 p_4 - p_6)Q_6, \end{aligned} \quad (24)$$

H_A corresponds to enzymatic activation of Cdh1 (reactions 4 to 6 in Table I),

$$H_A(p, Q) = k_1 p_7 (p_5 - p_1 p_3) Q_1 Q_3 Q_7 + k_2 p_7 (p_1 p_3 - p_5) Q_5 Q_7$$
$$+ k_3 p_7 (p_2 p_3 - p_5) Q_5 Q_7, \tag{25}$$

and, finally, H_B, which corresponds to synthesis and degradation of CycB, is given by (reactions 7 and 8 in Table I),

$$H_B(p, Q) = k_7 (p_7 - 1) + k_8 (1 - p_7) Q_7$$
$$+ k_8 a p_1 (1 - p_7) Q_1 Q_7. \tag{26}$$

We now proceed to apply the procedure explained in Section II in order to obtain the SCQSSA for the system determined by the transition rates given in Table I. We first need to determine which of the variables are slow variables and which ones are fast variables. As shown in Table II, the pairs (p_1, Q_1), (p_2, Q_2), and (p_7, Q_7), corresponding to the active and inactive forms of Cdh1 and to CycB, respectively, are the slow generalised coordinates, as the generalised positions scale with s_0. The remaining generalised coordinates scale as e_0 and, therefore, are fast variables. Furthermore, the rescaled Hamiltonian is given by

$$H_k(p, Q) = k_1 E S^2 H_\kappa(p, q), \tag{27}$$

where

$$H_\kappa(p, q) = H_{\kappa, A} + H_{\kappa, I} + H_{\kappa, B}, \tag{28}$$

with

$$H_{\kappa, I} = \kappa_4 (p_6 - p_2 p_4) q_2 q_4 + \kappa_5 (p_2 p_4 - p_6) q_6$$
$$+ \kappa_6 (p_1 p_4 - p_6) q_6,$$
$$H_{\kappa, A} = p_7 (p_5 - p_1 p_3) q_1 q_3 q_7 + \kappa_2 p_7 (p_1 p_3 - p_5)$$
$$\times q_5 q_7 + \kappa_3 p_7 (p_2 p_3 - p_5) q_5 q_7, \tag{29}$$
$$H_{\kappa, B} = \kappa_7 (p_7 - 1) + \kappa_8 (1 - p_7) q_7$$
$$+ \kappa_8 \alpha p_1 (1 - p_7) q_1 q_7.$$

The rescaled parameters κ_i are given in Table II. Last, by rescaling time and defining the dimensionless time variable as $\tau = k_1 E S t$ (Table II), SCQSSA equations (17), (18), (21), and (22) lead to (see Ref. 38 for a detailed derivation),

$$\frac{dq_1}{d\tau} = p_4 p_{e_4} \frac{\kappa_6 q_2}{q_2 + J_2} - p_7 p_3 p_{e_3} \frac{\kappa_3 q_7 q_1}{q_1 + J_1} + \kappa_8 \alpha (1 - p_7) q_7 q_1, \quad (30)$$

$$\frac{dq_2}{d\tau} = - p_4 p_{e_4} \frac{\kappa_6 q_2}{q_2 + J_2} + p_7 p_3 p_{e_3} \frac{\kappa_3 q_7 q_1}{q_1 + J_1}, \quad (31)$$

$$\frac{dq_7}{d\tau} = \kappa_7 - \kappa_8 (1 + \alpha p_1 q_1) q_7, \quad (32)$$

$$p_5 = p_3 p_1, \quad (33)$$

$$p_6 = p_4 p_2, \quad (34)$$

$$\frac{dp_7}{d\tau} = - (1 - p_7) \kappa_8 (1 + \alpha p_1 q_1), \quad (35)$$

where $p_1 = p_2$, p_3, and p_4 are constants to be determined and $J_1 = \kappa_2 + \kappa_3$ and $J_2 = k_4^{-1}(k_5 + k_6)$, and $p_{e3} = e_3/E$ and $p_{e4} = e_4/E$. Note that for $q_1(\tau) + q_2(\tau) = p_c$, with $p_c = s_0/S$, to hold $p_7 = 1$ must be satisfied. In this case, we have

$$\frac{dq_1}{d\tau} = p_4 p_{e_4} \frac{\kappa_6 (p_c - q_1)}{(p_c - q_1) + J_2} - p_3 p_{e_3} \frac{\kappa_3 m q_7 q_1}{q_1 + J_1}, \quad (36)$$

$$\frac{dq_7}{d\tau} = \kappa_7 - \kappa_8 (1 + \alpha p_1 q_1) q_7, \quad (37)$$

$$p_5 = p_3 p_1, \quad (38)$$

$$p_6 = p_4 p_1. \quad (39)$$

As shown in Ref. 38, the parameter values are determined by comparing the corresponding mean-field approximation, which is obtained by taking $p_i = 167$ and $p_c = p_{e3} = p_{e4} = 1$, i.e., the total number of molecules of Cdh1 and its activating and inhibiting enzymes be exactly equal to its average, i.e., $s_0 = S$ and $e_3 = e_4 = E$, to the system originally proposed by Tyson and Novak.22 In Eq. (36), we have redefined $\kappa_3 \to \kappa_3 m$ in order to make explicit the dependence on the bifurcation parameter, m, as used by Tyson and Novak.22 The parameter values are shown in Table III.

Upon rescaling of the variables (Table II) and the Hamiltonian (Eq. (15)), the action functional reads

$$S(p, q) = s_0 \int_0^\tau \left(-H_\kappa(p, q) - \sum_{slow} q_i \frac{dp_i}{ds} - \sum_{fast} q_j \, \epsilon \, \frac{dp_j}{ds} \right) ds + \sum_i^n S_{0,i}(p_i). \quad (40)$$

It is straightforward to check that in SCQSSA conditions $H_\kappa(p,q) = 0$. Furthermore, since $p_1 = p_2 = \text{const.}$ and $p_7 = 1$, and $\epsilon \dot{p}_j \simeq 0$ for the fast generalised coordinates, the SCQSS approximation of the action Eq. (40), S_{QSS}, reduces to

$$S_{QSS}(p) = \sum_{i=1}^n S_{0,i}(p_i), \quad (41)$$

where, as per the SCQSSA, p_5 and p_6 are determined by Eqs. (38) and (39), respectively, $p_7 = 1$, which implies $S_{0,7}(p_7) = 0$ and $p_1 = p_2$, p_3, and p_4 are constants that remain to be determined. In order to do so, we resort to the method developed in Ref. 38. The quasi-steady state characteristic function, $G_{QSS}(p, \tau)$, is given by

$$G_{QSS}(p, \tau) = e^{\left(-\sum_{i=1}^6 S_{0,i}(p_i) \right)} = \prod_{i=1}^6 G_{0,i}(p_i), \quad (42)$$

where $G_{0,i}(p_i) = e^{-S_{0,i}(p_i)}$ is the generating function of the probability distribution for the initial condition of species X_i $i = 1, \ldots, 6$. In Ref. 38, we have shown that, applying a Laplace-type asymptotic method71,72 to the integrals,

$$P(X_1(\tau = 0) = s_0) = \frac{1}{2\pi i} \oint_C \frac{G_{0,1}(p_1)}{p_1^{s_0+1}} dp_1$$

$$= \frac{1}{2\pi i} \oint_C \frac{e^{-\left(S_{0,1}(p_1) + s_0 \log p_1\right)}}{p_1} dp_1, \quad (43)$$

$$P(X_i(\tau = 0) = e_i) = \frac{1}{2\pi i} \oint_C \frac{e^{-\left(S_{0,i}(p_i) + e_0 \log p_i\right)}}{p_i} dp_i$$

$$\text{with } i = 3, 4,$$

where $p_1 = p_2$, p_3, and p_4 can be given as functions of s_0 and e_i, $i = 3, 4$, i.e., the initial numbers of Cdh1 molecules and Cdh1-inactivating and Cdh1-activating enzymes, respectively,

$$-p_1 \frac{dS_{0,1}}{dp_1} = s_0,$$

$$\quad (44)$$

$$-p_i \frac{dS_{0,i}}{dp_i} = e_i \text{ for } i = 3, 4.$$

$P(X_1(\tau = 0) = s_0)$, $P(X_3(\tau = 0) = e_3)$, and $P(X_4(\tau = 0) = e_4)$ are the probabilities that X_1 initially takes the value $X_1(\tau = 0) = s_0$ and that X_3 and X_4 have initial values $X_3(\tau = 0) = e_3$ and $X_4(\tau = 0) = e_4$. These probabilities can be interpreted to correspond to variability in the abundance of these enzymes within a population of cells. A particularly simple case results from assuming that $P(X_1(\tau = 0) = s_0)$, $P(X_3(\tau = 0) = e_3)$, and $P(X_4(\tau = 0) = e_0)$ are Poisson distributions with parameters S and E, respectively. In this case,[38]

$$p_1 = \frac{s_0}{S},$$

$$p_3 = \frac{e_3}{E}, \quad (45)$$

$$p_4 = \frac{e_4}{E}.$$

Note that, in the particular case in which the total numbers of Cdh1 and enzyme molecules are random Poisson variables, we have that $p_1 = p_c$, $p_3 = p_{e3}$, and $p_4 = p_{e4}$.

A   Bifurcation analysis

Fig. 2 shows results regarding the bifurcation behaviour of the SCQSS approximation of the stochastic bistable enzyme-catalysed system Eqs. (36)-(39). In particular, we are interested in a comparison between the bistable behaviour of the mean-field model, corresponding to

taking $p_i = 1$ for all i, and that of the SCQSS approximation with p_1, p_3, and p_4 given by Eq. (44), i.e., they are determined as functions of s_0 and e_0.

We have shown that both the ratios of p_3 and p_4, $\rho = \dfrac{p_3 p e_3}{p_4 p e_4} = \dfrac{p_3^2}{p_4^2} = \dfrac{e_3^2}{e_4^2}$, and p_1 alter the

bistable behaviour of the system beyond the predictions of the mean-field model. In particular, we observe that decreasing the value of ρ extends the region of stability of the G_1-fixed point, i.e., the fixed point corresponding to the steady-state value of q_1, such that $q_1 \sim$ 1. By contrast, when ρ is increased, the stability region of the G_1-fixed point shrinks. Intuitively, given the relation between p_3 and p_4 and the number of Cdh1-inactivating and Cdh1-activating enzyme, this result is straightforward to interpret: decreasing the number of Cdh1-inactivating enzyme demands a larger value of m in order to de-stabilise the G_1-fixed point. This is fully confirmed by direct simulation using Gillespie stochastic simulation algorithm.[54] Fig. 3 shows simulation results in which we compute the probability $P(x_1, T) =$ Prob$(x_1(\tau = T))$ for different values of ρ 1. T has been chosen so that the system has reached steady state conditions. We observe, that for $\rho = 1$ and $m = 0.3$, the system evolves towards the $q_1 \ll$ 1-fixed point (i.e., the S-G_2-M fixed point). As ρ decreases, i.e., there is more Cdh1-inactivating enzyme than Cdh1-activating enzyme, the system enters the bistable regime. If ρ reaches low-enough values (depending upon the initial condition), we may even observe an exchange of stability, i.e., the system evolves towards the $q_1 \sim$ 1-fixed point.

Regarding the dependence on p_1, we have checked the predictions of the SCQSS approximation by means of simulations with different values of s_0. Figure 2 shows the bi-stability region of system Eqs. (36)-(39) in p_1–m_R-space, where $m_R = \rho m$. For a fixed value of m_R, there is a threshold value for p_1 below which the system stops being bistable to become entrapped into the S-G_2-M fixed point (i.e., $q_1 \ll$ 1). In order to validate this prediction, we have conducted stochastic simulations for different values of s_0. Figure 4 shows simulation results for $P(x_1, T) = $ Prob$(x_1(\tau = T))$. We observe that for small values of s_0, the system is locked into the S-G_2-M fixed point, as predicted by the SCQSS approximation. As s_0 increases, the system enters a fluctuation-dominated bistable regime where, as the system goes through the bifurcation point, the system undergoes bistable behaviour. This behaviour is typical in a system undergoing a phase transition, where fluctuations unboundedly increase.[73] Finally, as s_0 continues to increase, the system becomes trapped into G_1-fixed point (see Figure 4). These results fully reproduce the behaviour predicted by our SCQSSA stability analysis.

The aforementioned behaviour regarding unbounded increase of fluctuations close to a bifurcation[73] is used to locate the critical value of the associated control parameter, i.e., ρ and p_c for the simulations shown in Figs. 3 and 4, respectively. This property allows us to do a quantitative comparison between the simulations and asymptotic analysis. To this end, we plot how the variance, $\sigma^2 = \langle (x_1 - \langle x_1 \rangle)^2 \rangle$, where $x_1 = X_1(\tau = T)/S$, changes as the corresponding control parameter varies. Regarding the results shown in Fig. 5(a) (associated to the simulations shown in Fig. 3), we observe that the critical value of the control parameter ρ, ρ_B, is approximately $\rho_B \simeq 0.7$, which, taking into account that $m = 0.3$, implies that the critical value of the renormalized mass, $m_R = \rho_m$, $m_B = \rho_B m \simeq 0.21$. Our asymptotic

analysis predicts that $m_B = 0.11$ (see Fig. 2(b) with $p_c = 1$). The results shown in Fig. 5(b) (corresponding to the simulations shown in Fig. 4), the critical value of p_c, p_B, is approximately $p_B \simeq 0.7$. The prediction of our asymptotic analysis (see Fig. 2(b) with $\rho = 1$) is $p_B = 0.6$.

IV Auto-Activation Gene Regulatory Circuit

We now proceed to analyse the effects of intrinsic noise in a model of a bistable self-activation gene regulatory circuit30,55,74 in the context of the quasi-steady regime. Many instances of genetic switches, i.e., bistable gene regulatory circuits, have been identified. 25,26,75–77 Most of them are characterised by the presence of a positive feedback in which one of the molecular species involved in the system upregulates its own production. All of these systems exhibit bi-stability and hysteresis, i.e., a form of memory associated to bistable systems, and some of them are thought to exist in regimes where stochastic switching is frequent.77,78 Noise effects on this kind of system have been extensively analysed and found to have both constructive and deleterious effects. For example, Frigola *et al.*30 have found that noise stabilises the inactive (OFF) steady-state of a model of a bistable self-activation gene regulatory circuit by extending its stability region. In this section, we analyse the effects of noise specifically associated to the quasi-steady state regime in the large-deviations (large number of molecules) limit.

We study the stochastic system of the simple self-activating gene regulatory circuit schematically represented in Fig. 6. In this circuit, the gene product binds to form dimers which then act as its own transcription factor by binding to the promoter region of the gene. The rate-limiting factor is therefore the number of available binding sites within the promoter of the gene. For simplicity, our stochastic model associated to the rates shown in Table IV does not explicitly account for dimer formation. We will assume that this process is very fast so it can be subsumed under the formation of transcription-factor dimer/promoter binding site trimers (reaction 3, Table IV). Furthermore, it is important to note that our stochastic dynamics exhibits a conservation law: $X_2 + X_3 = e_0$ at all time. This conservation law expresses the fact that the total number of binding sites, e_0, is constant.

In order to proceed with our analysis of the stochastic model of self-activated gene regulation (see Table IV and Fig. 6), we apply the general methodology associated to our SCQSS approximation. Following the general procedure explained in Secs. I–III, we start by deriving the stochastic Hamiltonian associated to the process defined by the transition rates shown in Table IV (see Section II),

$$H(p, Q) = (p_1 - 1)(\hat{R} + k_1 Q_2 p_2) + k_2(1 - p_1)Q_1 + k_3(p_2 - p_1^2 p_3)Q_1^2 Q_3 + k_4(p_1^2 p_3 - p_2)Q_2,$$

(46)

which, according to our theory (see Section II), gives rise to the re-scaled Hamiltonian, $H_\kappa(p, q)$, defined by

$$H_\kappa(p, q) = (p_1 - 1)(R + \kappa_1 q_2 p_2) + \kappa_2(1 - p_1)q_1 + (p_2 - p_1^2 p_3)q_1^2 q_3 + \kappa_4(p_1^2 p_3 - p_2)q_2, \quad (47)$$

where $H(p, Q) = k_3 ES^2 H_\kappa(p, q)$ and the re-scaled variables, q_i, and re-scaled rate constants, κ_j, are defined in Table V. The re-scaled Hamilton equations are thus given by

$$\frac{dq_1}{d\tau} = R + \kappa_1 q_2 p_2 - \kappa_2 q_1 - 2q_1^2 q_3 p_1 p_3 + 2\kappa_4 p_1 p_3 q_2, \quad (48)$$

$$\epsilon\frac{dq_2}{d\tau} = (p_1 - 1)\kappa_1 q_2 + q_1^2 q_3 - \kappa_4 q_2, \quad (49)$$

$$\epsilon\frac{dq_3}{d\tau} = -q_1^2 q_3 p_1^2 + \kappa_4 p_1^2 q_2, \quad (50)$$

$$\frac{dp_1}{d\tau} = \kappa_2(p_1 - 1) - 2q_1 q_3(p_2 - p_1^2 p_3), \quad (51)$$

$$\epsilon\frac{dp_2}{d\tau} = \kappa_1(1 - p_1)p_2 - \kappa_4(p_1^2 p_3 - p_2), \quad (52)$$

$$\epsilon\frac{dp_3}{d\tau} = q_1^2(p_1^2 p_3 - p_2). \quad (53)$$

From these equations, we observe that for $q_2(\tau) + q_3(\tau) = p$, where $p = e_0/E$, to hold we must have that $p_1(\tau) = 1$ for all τ. Imposing this condition on Eq. (51) implies that $p_2(\tau) = p_3(\tau)$, which, in turn, together with Eqs. (52) and (53), imply that $p_2 = p_3 = \text{const}$. Finally, applying the QSS approximation to remaining equations, Eqs. (48)-(50), we obtain

$$\frac{dq_1}{d\tau} = R + \kappa_1 p p_2 \frac{q_1^2}{\kappa_4 + q_1^2} - \kappa_2 q_1, \quad (54)$$

$$q_2 = p - q_3 = p\frac{q_1^2}{\kappa_4 + q_1^2}. \quad (55)$$

As for the bistable enzyme-catalysed system, the parameter values are determined by matching the mean-field limit of our stochastic model, which is obtained by setting $p_i = 1$ for all $i \ne 7$ and $p = 1$ (i.e., the number of binding sites exactly equal to its average), to the mean-field system proposed by Frigola *et al.*[30] The mapping of our parameters to those of Ref. 30 and their associated values is given in Table VI.

Finally, according to the theory developed in Section II, p_2 is determined in terms of the total number of binding sites within the gene promoter, e_0,

$$-p_2\frac{dS_0}{dp_2} = e_0, \quad (56)$$

where $S_0(p) = \ln(G_0(p))$ and $G_0(p)$ is the generating function associated to the probability distribution of e_0, $P(e_0)$. This probability distribution can be interpreted as corresponding to the distribution over a cell population of the number of binding sites in the promoter of gene x_1. For example, if $P(e_0)$ is a Poisson distribution, the Eq. (56) reads[38]

$$p_2 = \frac{e_0}{E}, \quad (57)$$

where $E \equiv \langle e_0 \rangle$, i.e., the average of e_0 over a population of cells. Therefore, according to this analysis, we have that $p = p_2$, provided that $P(e_0)$ is a Poisson distribution with parameter E.

A Bifurcation analysis

Fig. 7 shows results regarding how the bifurcation diagram varies as we change $pp_2 = p_2^2$, which, we recall, is determined by the (probability distribution of the) total number of binding sites within the gene promoter. Inspection of Eq. (54) shows that p_2 has the effect of renormalising the self-activation rate κ_1. If $p_2^2 < 1$, then the rate of gene self-activation is effectively reduced, and consequently, the stability region of the inactive steady-state, $q_1 \sim 0$, is extended. That is, we need to go to larger values of κ_4 to enter the region where the active steady-state, $q_1 > 1$, becomes stable (see Fig. 7). On the contrary, $p_2^2 > 1$ has the effect of extending the stability region of the active steady-state, $q_1 > 1$.

In order to verify the predictions of our bifurcation analysis (Fig. 7), we consider Eqs. (56) and (57), which relate the momentum variable p_2 to the number of binding sites within the gene promoter. If we assume that the latter is distributed according to a Poisson distribution, then Eq. (57) holds and $p_2 = p = e_0/E$. Under these conditions, our bifurcation analysis

predicts that the probability distribution of X_1, i.e., the random variable associated to the generalised coordinate q_1, should change, as e_0 decreases, from being uni-modal with a single maximum about the ON value of X_1 (or, when scaled with s_0, q_1) to exhibiting bi-modality, as the system approaches the saddle-node bifurcation which annihilates the ON state as it collides with the saddle point, with two peaks about the ON and OFF states. If e_0 is further reduced, the system will be driven passed this saddle-node bifurcation, the probability distribution becomes uni-modal but, unlike its large e_0 counterpart, its peak is about the OFF q_1-steady-state. We have verified this prediction by running simulations using the SSA. The results, which agree with our prediction, are shown in Fig. 8.

Quantitative comparison between our asymptotic analysis and the simulation results follows the same procedure as in Section III, i.e., we look at how the variance aforementioned behaviour regarding unbounded increase of fluctuations close to a bifurcation[73] is used to locate the critical the variance $\sigma^2 = \langle (x_1 - \langle x_1 \rangle)^2 \rangle$, with $x_1 = X_1(\tau = T)/S$ changes as the control parameter varies: the maximum of σ^2 as a function of the control parameter corresponds to the critical value. According to Fig. 9(b), the critical value of p, p_B, is approximately given by $p_B \simeq 0.7$. Our asymptotic analysis (see Fig. 9(b)) predicts that $p_B = 0.78$.

V Conclusions and Discussion

By means of the semi-classical quasi-steady state approximation, Section II, we have analysed stochastic effects affecting the onset of bi-stability in cell regulatory systems. Our theory shows that there exists a conserved momentum coordinate associated to each conserved chemical species. In the case of the enzyme-catalysed bistable system, Section III, there are three such conserved momenta, associated to each of the conserved chemical species, i.e., Cdh1 and its activating and inhibiting enzymes. For the self-activation gene regulatory network, we have one conserved momentum, corresponding to conservation of the number of binding sites of the gene's promoter region.

According to the SCQSSA analysis of Ref. 38, the maximum rate achieved by an enzymatic reaction, V_{max}, predicted by the mean-field theory[29] is renormalised by a factor which equals the value of the (constant) momentum coordinate p_i associated to the conserved enzyme: $V_{max}^{(SC)} = p_{ej} p_i V_{max}$ where $V_{max}^{(SC)}$ is the maximum rate predicted by the SCQSSA. Similarly, we have shown that the mean-field maximum activation rate associated to the auto-activation gene regulatory model, A_{max}, is renormalised in the presence of noise by a factor equal to the conserved momentum coordinate corresponding to the number of binding sites in the gene promoter, p_2, i.e., $A_{max}^{(SC)} = p p_2 A_{max}$, with $A_{max}^{(SC)}$ being the SCQSSA maximum activation rate. As a consequence of this parameter renormalisation, we have shown that variation in the value of the conserved momenta can trigger bifurcations leading to the onset of bistable behaviour beyond the predictions of the mean-field limit, i.e., for values of parameters where the mean-field limit predicts the system to be mono-stable, the SCQSSA predicts bi-stability, and vice versa (see Figs. 2 and 7).

Furthermore, we have established that the value of the constant momenta is actually determined by the probability distribution of the associated conserved chemical species, and, ultimately, by the number of molecules of these species (see Eqs. (44), (56), and (57)). Therefore, our theory establishes that the numbers of molecules of the conserved species are order parameters whose variation should trigger (or cancel) bistable behaviour in the associated systems. This prediction is fully confirmed by direct numerical simulation using the stochastic simulation algorithm (see Figs. 3, 4, and 8). Quantitative comparison between the predictions of our asymptotic analysis and the simulation results (see Figs. 5 and 9) shows that our theoretical approach slightly underestimates the critical value for the bistable enzyme-regulated system. The theoretical prediction for the self-activating gene regulatory network appears to slightly overestimate the critical value.

Our results allow us to propose a means of controlling cell function. For example, regarding the enzyme-catalysed bistable model analysed in Section III, varying the number of molecules of the three conserved chemical species (Cdh1 and the associated activating and inhibiting enzymes) enables us to lock the system into either of the G_1 or the S-G_2-M stable fixed points or to drive the system into its bistable regime where random fluctuations will trigger switching between these two states. This could be accomplished by ectopically increasing the synthesis of the corresponding molecule or by targeting the enzymes with enzyme-targeted drugs.[79,80] Similarly, the dynamics of the self-activating gene regulatory system could be driven into or out of its bistable regime by supplying an inhibitor that irreversibly binds to the promoter region, thus decreasing the effective number of binding sites.

This result allows us to explore strategies, for example, in the field of combination therapies in cancer treatment. Cellular quiescence is a major factor in resistance to unspecific therapies, such as chemo- and radio-therapy, which target proliferating cells. Bi-stability is central to control cell-cycle progression and to regulate the exit from quiescence, with enzyme catalysis (usually accounted for by (mean-field) Michaelis-Menten, quasi-steady state dynamics) being ubiquitously involved.[25,26,28,77] Our findings will allow us to formulate combination strategies in which chemo- or radio-therapy is combined with a strategy aimed at driving cancer cells into proliferation or quiescence depending on the phase of the treatment cycle. Evaluation of the viability and efficiency of such combination require the formulation of multi-scale models[70,81] whose analysis is beyond this scope of this paper, and it is therefore postponed for future work.

Our approach differs from previous work, such as Dykman *et al.*[82] in a significant aspect, namely, whilst their aim is to estimate the rate of noise-induced transition between metastable states in systems exhibiting multi-stability, the purpose of our analysis is to ascertain whether noise can alter the multi-stability status of the system. Dykman *et al.*[82] do not address such issue.

Eqs. (36)-(39), (54), and (55) are derived from a semi-classical approximation of the master equation (or its equivalent description in terms or the generating function PDE). This approximation yields a set Hamilton equations (Eqs. (8) and (9)) whose solutions are the optimal fluctuation paths and, as such, they describe fluctuation-induced phenomena which

cannot be accounted for by the mean-field approximation. One of the best known examples of this is exit problems from metastable states in noisy systems (e.g., extinctions), where the semi-classical approximation provides the optimal escape path from which information such as mean-first passage time or waiting time for extinction can be obtained (see, for example, Refs. 63, 67, and 83). Furthermore, Eqs. (36)-(39), (54), and (55) are derived from the general Hamilton equations, Eqs. (8) and (9), by means of an approximation based on separation of time scales, not on any mean-field assumption.

A closely related subject to that analysed in this paper is that of noise-induced bifurcations. 31 Such phenomenon has been studied in biological systems where the mean-field limit does not predict bistability, such as the so-called enzymatic futile cycles32 where noise associated to the number of enzymes induces bistability. In the absence of this source of noise, the system does not exhibit bistable behaviour. We have not dealt with such noise-induced phenomena in the present paper, in the sense that all the systems analysed in this paper are such that their mean-field limit exhibits bistability. We leave the interesting issue of whether our SCQSSA framework can be used to analyse noise-induced bifurcation phenomena for future research.

Acknowledgments

References

1. Kepler TB, Elston TC. Biophys J. 2001; 81:3116. [PubMed: 11720979]

2. Kaern M, Elston TC, Blake WJ, Collins JJ. Nat Rev Genet. 2005; 6:451. [PubMed: 15883588]

3. Maheshri N, O'Shea EK. Annu Rev Biophys Biomol Struct. 2007; 36:413. [PubMed: 17477840]

4. Losick R, Desplan C. Science. 2008; 320:65. [PubMed: 18388284]

5. Raj A, van Oudenaarden A. Cell. 2008; 135:216. [PubMed: 18957198]

6. Cai L, Dalal CK, Elowitz MB. Nature. 2008; 455:485. [PubMed: 18818649]

7. Eldar A, Elowitz MB. Nature. 2010; 467:167. [PubMed: 20829787]

8. Kussell E, Leibler S. Science. 2005; 309:2075. [PubMed: 16123265]

9. Acar M, Mettetal JT, van Oudenaarden A. Nat Genet. 2008; 40:471. [PubMed: 18362885]

10. Guerrero P, Byrne HM, Maini PK, Alarcon T. From invasion to latency: intracellular noise and cell motility as key controls of the competition between resource-limited cellular populations. J Math Biol.

11. MacArthur BD, Please CP, Oreffo ROC. PLoS One. 2008; 3:e3086. [PubMed: 18769478]

12. Balazsi G, van Oudenaarden A, Collins JJ. Cell. 2011; 144:910. [PubMed: 21414483]

13. Cinquin O, Demongeot J. J Theor Biol. 2005; 233:391. [PubMed: 15652148]

14. Jaeger J, Monk N. J Physiol. 2014; 592:2267. [PubMed: 24882812]

15. Kauffman, SA. The Origins of Order. Oxford University Press; New York, USA: 1993.

16. Huang S. BioEssays. 2012; 34:149. [PubMed: 22102361]

17. Tyson JJ, Chen KC, Novak B. Curr Opin Cell Biol. 2003; 15:221. [PubMed: 12648679]

18. Legewie S, Bluthgen N, Herzel H. PLoS Comput Biol. 2006; 2:e120. [PubMed: 16978046]

19. Legewie S, Bluthgen N, Herzel H. Biophys J. 2007; 93:2279. [PubMed: 17526574]

20. Kalmar T, Lim C, Hayward P, Munoz-Descalzo S, Nichols J, Garcia-Ojalvo J, Martinez-Arias A. PLoS Biol. 2009; 7:e1000149. [PubMed: 19582141]

21. Ferrel JE, Xiong W. Chaos. 2001; 11:227. [PubMed: 12779456]

22. Tyson JJ, Novak B. J Theor Biol. 2001; 210:249. [PubMed: 11371178]

23. Gerard C, Goldbeter A. Proc Natl Acad Sci U S A. 2009; 106:21643. [PubMed: 20007375]

24. Gerard C, Goldbeter A. Front Physiol. 2012; 3:413. [PubMed: 23130001]

25. Yao G, Lee TJ, Mori S, Nevins JR, You L. Nat Cell Biol. 2012; 7:476.

26. Yao G. Interface Focus. 2014; 4:20130074. [PubMed: 24904737]

27. Gerard C, Goldbeter A. Interface Focus. 2014; 4:20130075. [PubMed: 24904738]

28. Bedessem B, Stephanou A. Math Biosci. 2014; 248:31. [PubMed: 24345497]

29. Keener, J, Sneyd, J. Mathematical Physiology. Springer-Verlag; New York, NY, USA: 1998.

30. Frigola D, Casanellas L, Sancho JM, Ibañes M. PLoS One. 2012; 7:e31407. [PubMed: 22363638]

31. García-Ojalvo, J, Sancho, JM. Noise in Spatially-Extended Systems. Springer-Verlag; 1999.

32. Samoilov M, Plyasunov S, Arkin AP. Proc Natl Acad Sci U S A. 2005; 102:2310. [PubMed: 15701703]

33. Rao CV, Arkin AP. J Chem Phys. 2003; 118:4999.

34. Turner TE, Schnell S, Burrage K. Comput Biol Chem. 2004; 28:165. [PubMed: 15261147]

35. Thomas P, Straube AV, Grima R. J Chem Phys. 2010; 133:195101. [PubMed: 21090871]

36. Dóka É, Lente G. J Chem Phys. 2012; 136:054111. [PubMed: 22320729]

37. Thomas P, Grima R, Straube AV. Phys Rev E. 2012; 86:041110.

38. Alarcón T. J Phys Chem. 2014; 140:184109.

39. Bruna M, Chapman SJ, Smith MJ. J Chem Phys. 2014; 140:174107. [PubMed: 24811625]

40. Burrage K, Tian T, Burrage P. Prog Biophys Mol Biol. 2004; 85:217. [PubMed: 15142745]

41. Vlachos DG. Adv Chem Phys. 2005; 30:1.

42. MacNamara S, Burrage K, Sidje RB. Multiscale Model Simul. 2008; 6:1146.

43. Cao Y, Gillespie DT, Petzold LR. J Comput Phys. 2005; 206:395.

44. Cao Y, Gillespie DT, Petzold LR. J Chem Phys. 2005; 122:014116.

45. Samant A, Vlachos DG. J Chem Phys. 2005; 123:144114. [PubMed: 16238381]

46. Liu WED, Vanden-Eijnden E. J Comput Phys. 2007; 221:158.

47. Sanft KR, Gillespie DT, Petzold LR. IET Syst Biol. 2011; 5:58. [PubMed: 21261403]

48. Rathinam M, Petzold LR, Cao Y, Gillespie DT. J Chem Phys. 2006; 10:12784.

49. Haseltine EL, Rawlings JB. J Chem Phys. 2002; 117:6959.

50. Salis H, Kaznessis Y. J Chem Phys. 2005; 122:054103.

51. Assaf M, Meerson B. Phys Rev E. 2006; 74:041115.

52. Newby J, Chapman J. Math Biol. 2013; 69:941.

53. Kang H-W, Kurtz TG. Ann Appl Probab. 2013; 23:529.

54. Gillespie DT. J Comput Phys. 1976; 22:403.

55. Assaf M, Roberts E, Luthey-Schulten Z. Phys Rev Lett. 2011; 106:248102. [PubMed: 21770603]

56. Bressloff, PC. Stochastic Processes in Cell Biology. Springer-Verlag; Berlin, Germany: 2014.

57. Kampen, NGV. Stochastic Processes in Physics and Chemistry. Elsevier; The Netherlands: 2007.

58. Kubo R, Matsuo K, Kitahara K. J Stat Phys. 1973; 9:51.

59. Alarcón T, Page KM. J R Soc Interface. 2007; 4:283. [PubMed: 17251148]

60. Touchette H. Phys Rep. 2009; 479:1.

61. Doi M. J Phys A: Math Gen. 1976; 9:1479.

62. Peliti L. J Phys France. 1985; 46:1469.

63. Assaf M, Meerson B, Sasorov PV. J Stat Mech. 2010

64. Gonze D, Halloy J, Gaspard P. J Chem Phys. 2002; 116:10997.

65. Feynman, RP, Hibbs, AR. Quantum Mechanics and Path Integrals. Dover Publications; Mineola, NY, USA: 2010.

66. Dickman R, Vidigal R. Braz J Phys. 2003; 33:73.

67. Elgart V, Kamenev A. Phys Rev E. 2004; 70:041106.

68. Täuber UC, Howard M, Vollmayr-Lee BP. J Phys A: Math Gen. 2005; 38:R79.

69. Briggs GE, Haldane JBS. Biochem J. 1925; 19:338. [PubMed: 16743508]

70. Guerrero P, Alarcón T. Math Modell Nat Phenom. 2015; 10:64.

71. Murray, JD. Asymptotic Analysis. Springer-Verlag; New York, NY, USA: 1984.

72. Ablowitz, MJ, Fokas, AS. Complex Variables. Introduction and Applications. Cambridge University Press; Cambridge, UK: 2003.

73. Goldenfeld, N. Lectures on Phase Transitions and the Renormalisation Group. Perseus Books Publishing; Reading, MA, USA: 1992.

74. Weber M, Buceta J. PLoS One. 2013; 8:e73487. [PubMed: 24039958]

75. Gardner TS, Cantor CR, Collins JJ. Nature. 1999; 403:339.

76. Ozbudak EM, Thattai M, Lim HN, Shraiman BI, van Oudenaarden A. Nature. 2004; 427:737. [PubMed: 14973486]

77. Lee TJ, Yao G, Bennett DC, Nevins JR, You L. PLoS Biol. 2010; 8:e1000488. [PubMed: 20877711]

78. Acar M, Becksei A, van Oudenaarden A. Nature. 2005; 435:228. [PubMed: 15889097]

79. Robertson JG. Biochem. 2005; 44:5561. [PubMed: 15823014]

80. Singh J, Petter RC, Baillie TA, Whitty A. Nat Rev Drug Discovery. 2012; 10:307.

81. Alarcón T, Byrne HM, Maini PK. Multiscale Model Simul. 2005; 3:440.

82. Dykman MI, Mori E, Ross J, Hunt PM. J Chem Phys. 1994; 100:5735.

83. Khasin M, Dykman MI. Phys Rev Lett. 2009; 103:068101. [PubMed: 19792614]

$$X_1 + X_3 \underset{k_2 X_7}{\overset{k_1 X_7}{\rightleftharpoons}} X_5 \xrightarrow{k_3 X_7} X_2 + X_3$$

$$X_2 + X_4 \underset{k_5}{\overset{k_4}{\rightleftharpoons}} X_6 \xrightarrow{k_6} X_1 + X_4$$

$$\varnothing \xrightarrow{k_7} X_7 \xrightarrow{k_8(1+aX_1)} \varnothing$$
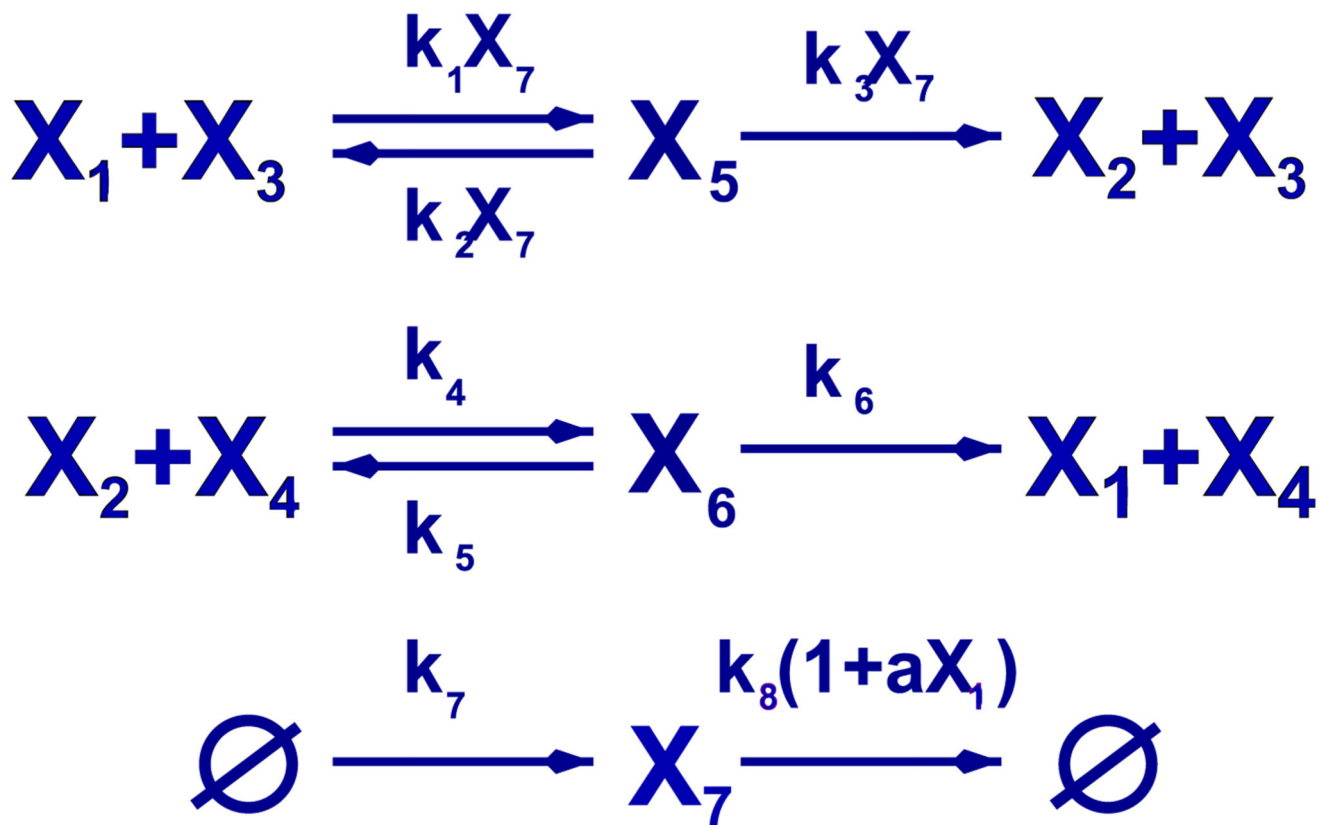
Fig. 1.

Reactions for the bistable enzyme-catalysed system proposed by Tyson and Novak.[22] X_1 represents active Cdh/Apc, X_2 inactive Cdh/Apc, X_3 inactivating enzymes, X_4 activating enzymes, X_5 active Cdh/Apc-inactivating-enzyme complexes, X_6 inactive Cdh/Apc-activating-enzyme complexes, and X_7 the number of CycB-CDK complexes. The first two reactions correspond to enzyme-catalysed inactivation and activation of Cdh/APC. The third reaction corresponds to the dynamics of CycB activity: synthesis at a constant rate, k_7, and degradation by natural decay and active Cdh/Apc-induced inactivation.
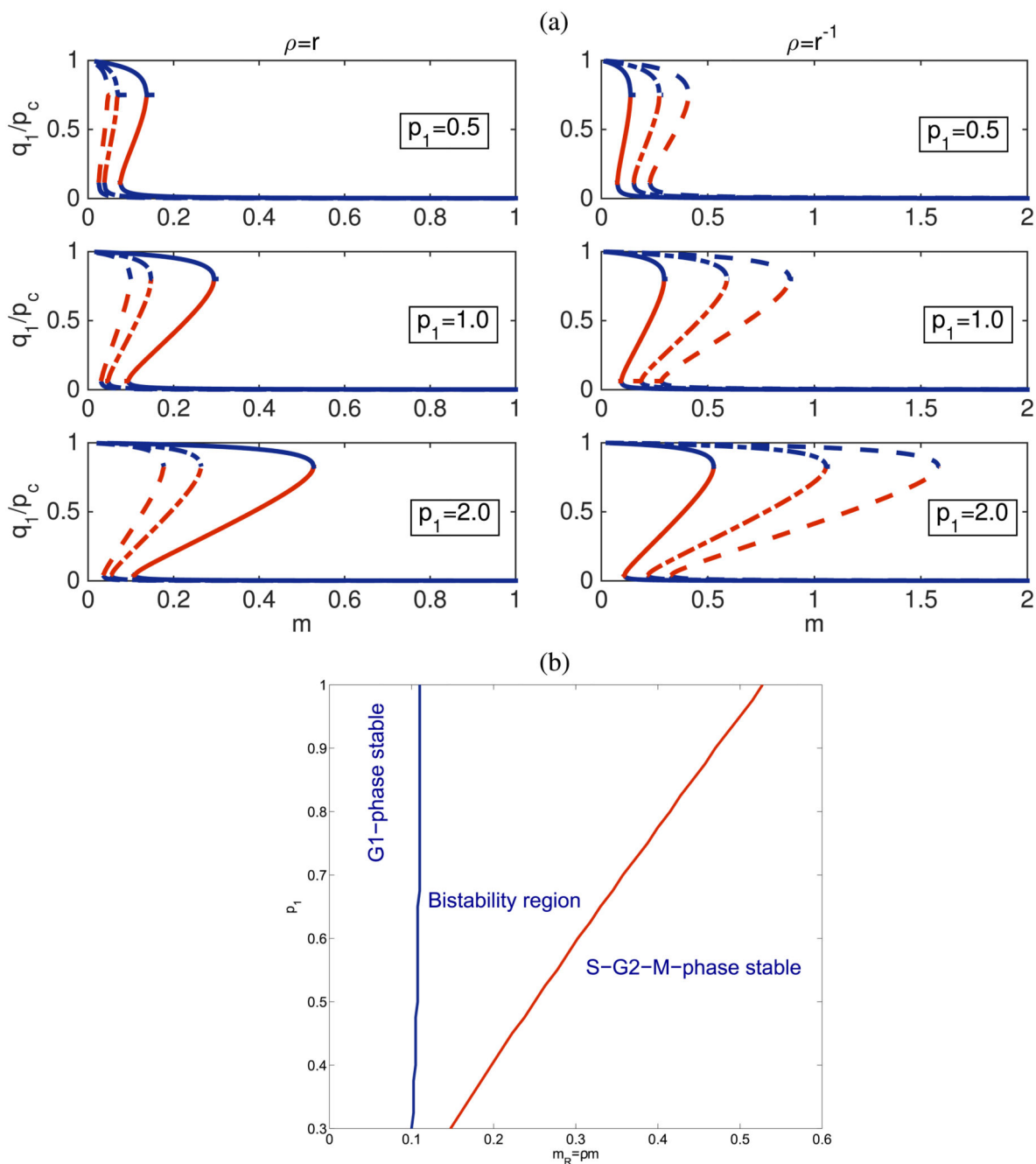
Fig. 2.

(a) Bifurcation analysis for the SCQSS approximation of the stochastic bistable enzyme-catalysed system Eqs. (36)-(39). The panels on the top plot (a) show the bifurcation diagrams for different values of the parameters p_1, $p_c = p_1$, and $\rho = \dfrac{p_3 p_{e_3}}{p_4 p_{e_4}}$. If e_0 and s_0 are random Poisson variables with parameter S and E, respectively, then $\rho = \dfrac{p_3^2}{p_4^2}$ (see Eq. (45)).

In these panels, solid lines correspond to $r = 1$, dotted-dashed lines to $r = 2$, and dashed lines to $r = 3$. The bottom plot (b) shows the bi-stability boundaries in $p_1 - m_R$ parameter space. The region between the boundaries corresponds to the bistable region of the stochastic Tyson and Novak system according to the SCQSS approximation.

mass=0.3, T=100, 1000 realizations, $(x_1(\tau=0), x_7(\tau=0))=(0.9, 0.1)$, S=1000, $\rho=X_4(\tau=0)/X_3(\tau=0)$
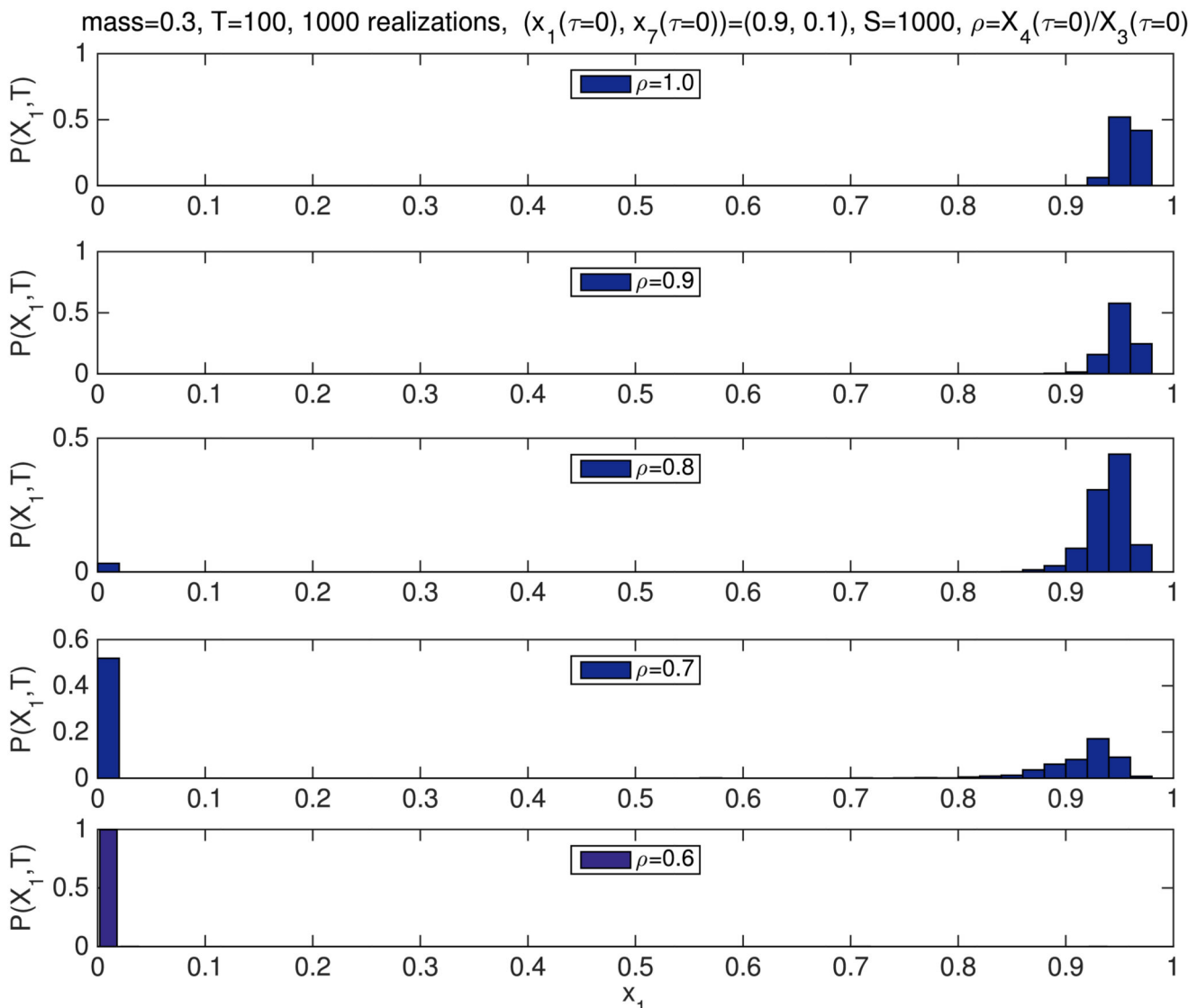
Fig. 3.

Simulation results for the stochastic bistable enzyme-catalysed system Table I. We have plotted the probability $P(x_1, T) = \text{Prob}(x_1(\tau = T))$, where $x_1 = X_1/S$ and $T = 100$ for different values of ρ. The initial number of Cdh1-inactivating and Cdh1-activating enzymes is fixed according to $X_3(t = 0) = \dfrac{e_0}{\rho}$ and $X_4(t = 0) = e_0$, respectively, $m = 0.3$. We aim to check our predictions regarding the effect of the ratio $\rho = \dfrac{p_3^2}{p_4^2} = \dfrac{e_3^2}{e_4^2}$ on the stability properties of the system. According to our results shown in Fig. 2, decreasing the ratio between the number of Cdh1-inactivating (e_4) and Cdh1-activating (e_3) enzymes, the system should be driven away from bistability and into the stable G_1-phase regime (see Fig. 2(b)). The remaining parameter values are inferred from those given by Tyson and Novak22 as shown in Tables II and III. We see that when varying ρ, the system switches from a state of high x_1 (ρ 0.9) to

a state of low x_1 (ρ 0.6), whereas at the intermediate levels (e.g., $\rho = 0.7$ and $\rho = 0.8$), the system is in a bistable state. We take $p_1 = p_c = 1$ in all the simulations shown in this figure. Average is performed over 1000 realisations.

mass=0.3, T=100, 1000 realizations, $(x_1(\tau=0), x_7(\tau=0))=(0.9, 0.1)$, S=1000
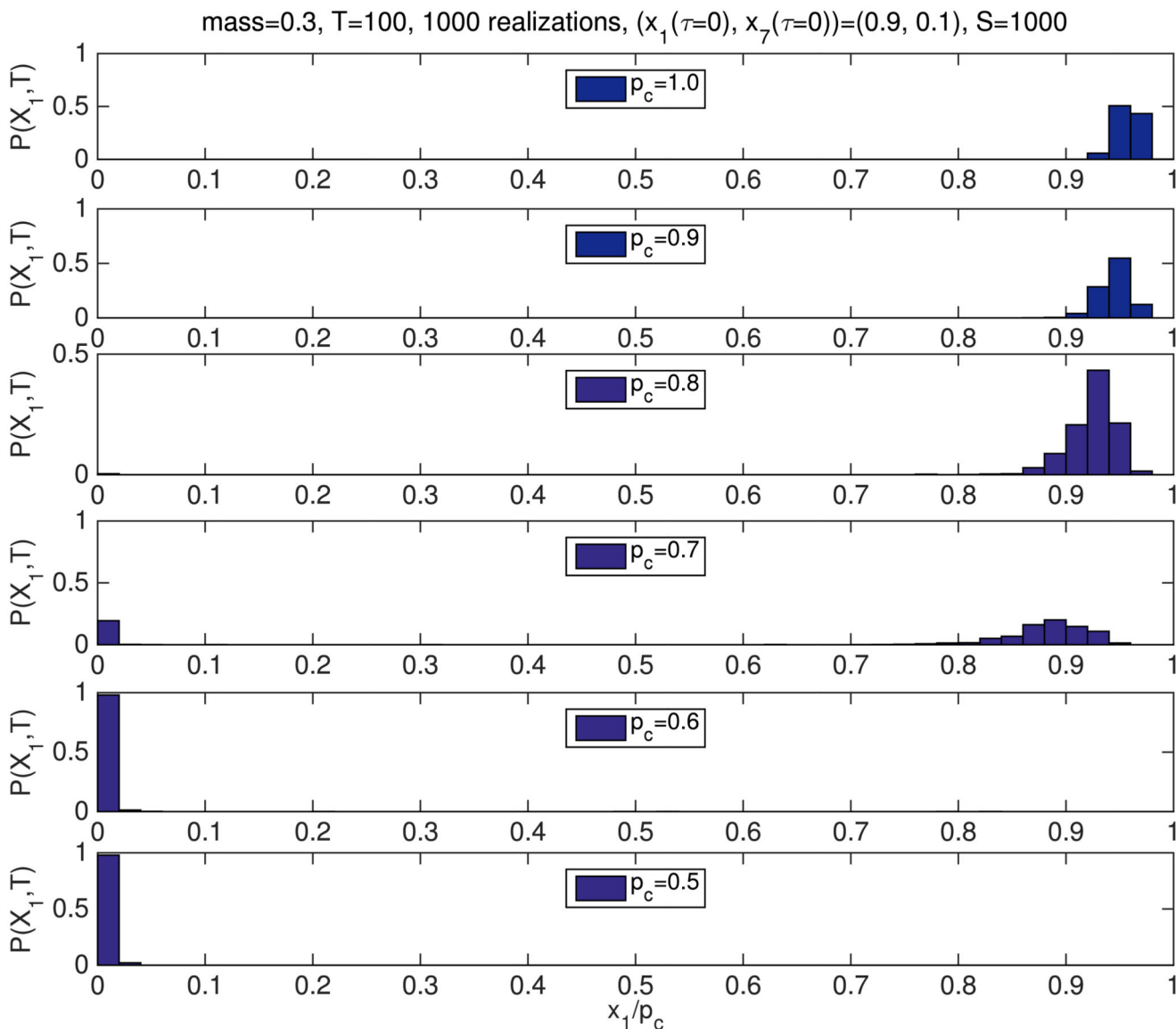
Fig. 4.

Simulation results for the stochastic bistable enzyme-catalysed system Table I. We have plotted the probability $P(x_1, T) = \text{Prob}(x_1(\tau = T))$, where $x_1 = x_1/S$ and $T = 100$ with different initial conditions and different values of p_c. Average is performed over 1000 realisations. $m = 0.3$ and $X_3(t = 0) = e_0$ and $X_4(t = 0) = e_0$. The remaining parameter values are inferred from those given by Tyson and Novak22 as shown in Tables II and III. We see that when varying p_c, the system switches from a state of high x_1 (p_c 0.8) to a state of low x_1 (p_c 0.6), whereas at the intermediate levels of $p_c = 0.7$, the system is in a bistable state.
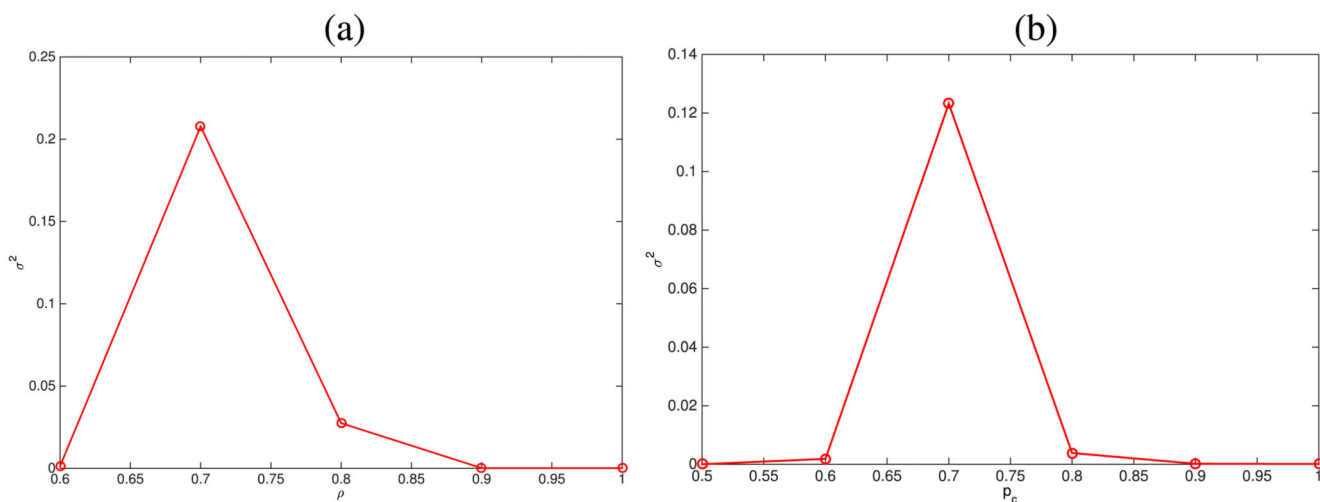
Fig. 5.

Plots showing the variance $\sigma^2 = \langle (x_1 - \langle x_1 \rangle)^2 \rangle$, where $x_1 = X_1(\tau = T)/S$ associated to the simulation results shown in Fig. 3 (panel (a)) and in Fig. 4 (panel (b)). These plots show how σ^2 changes as the control parameter (ρ, for the simulations associated to plot (a), and p_c for the simulations shown in plot (b)). The maximum of σ^2 as a function of the control parameter helps us to quantitatively determine the corresponding critical value.[73]
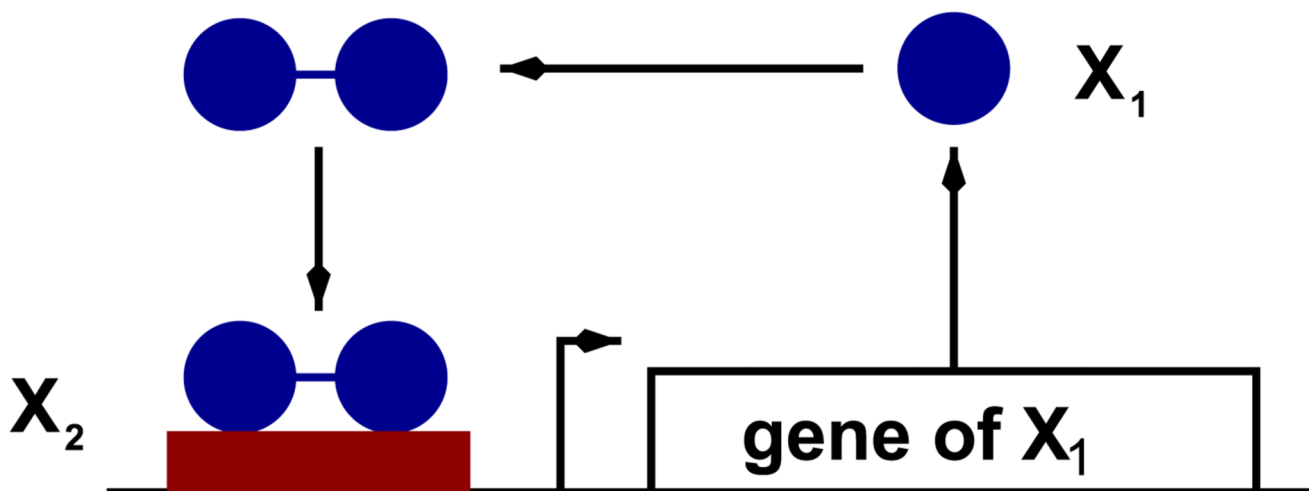
Fig. 6.
Schematic representation of the self-activating gene regulatory circuit. The gene product X_1 is its own transcription factor which, upon dimerisation, binds the promoter region of the gene thus triggering gene transcription. The transition rates corresponding to this gene regulatory circuit are given in Table IV. For simplicity, we use an effective model in which the formation of the dimer and binding to the promoter region are taken into account in a single reaction, and the resulting number of promoter sites bound by two transcription factors is denoted as X_2.
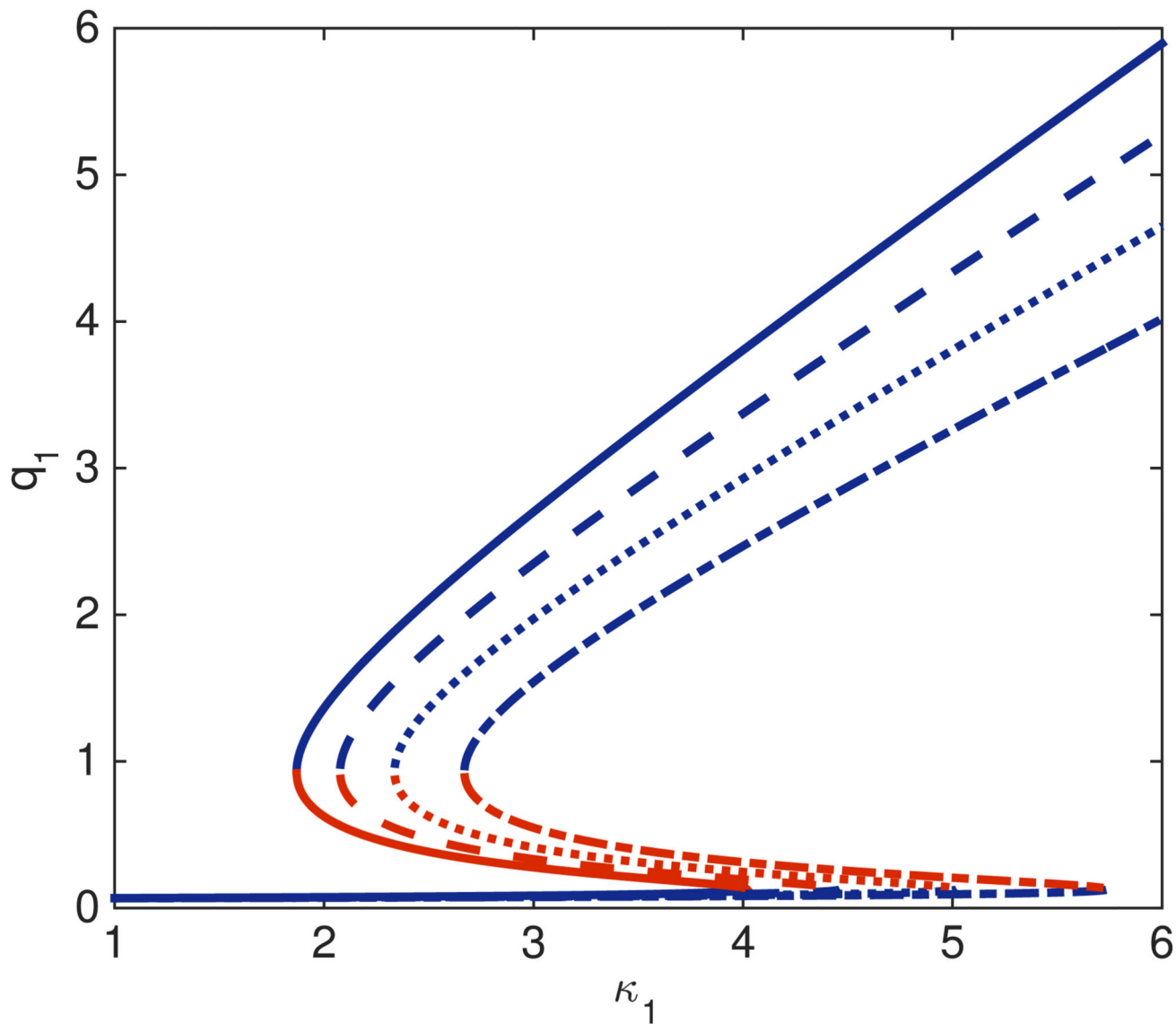
Fig. 7.
Bifurcation analysis for the SCQSS approximation of the stochastic auto-activation gene regulatory circuit Eqs. (54) and (55). This figure shows the bifurcation diagram for different values of the parameters of p_2. In these, solid lines correspond to $p_2^2 = 1$, dashed lines to $p_2^2 = 0.9$, dotted to $p_2^2 = 0.8$, and dashed-dotted lines to $p_2^2 = 0.7$ (recall that $p_2 = p$). Parameter values as given in Table VI.
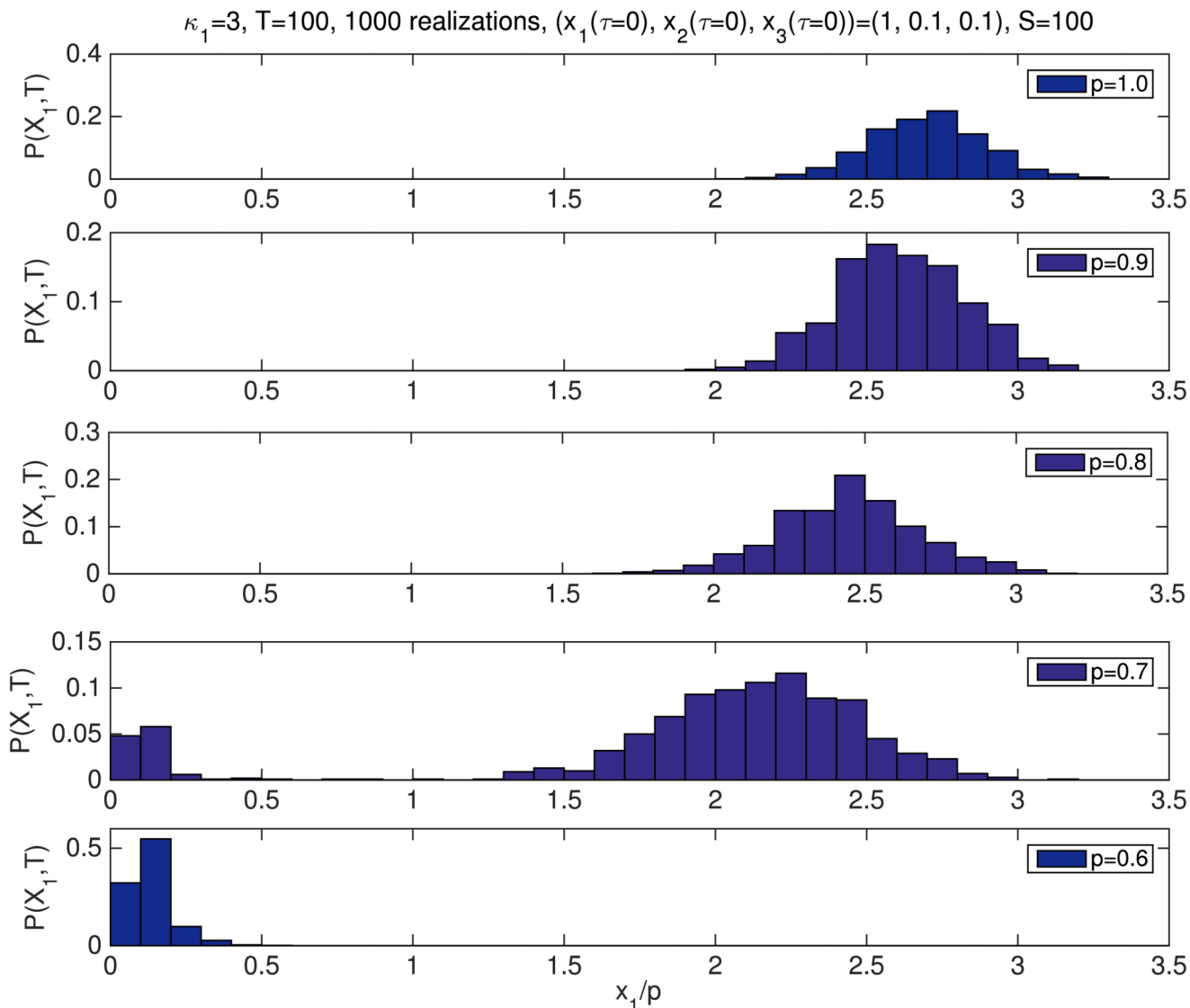
Fig. 8.
Simulation results for the stochastic gene regulatory circuit of self-activation (Table IV). We have plotted the probability $P(x_1, T) = \text{Prob}(x_1(\tau = T))$, where $x_1 = X_1/S$ and $T = 100$ as the number of binding sites in the gene promoter, given by $X_3(t = 0) = p E$. Average is performed over 1000 realisations. Parameter values are inferred from those given by Frigola *et al.*30 as shown in Tables V and VI. We see the emergence of bistability at $p = 0.7$, whereas for smaller(larger) values of p, the system will be in the stable steady state corresponding to low(high) number of transcription factor molecules.
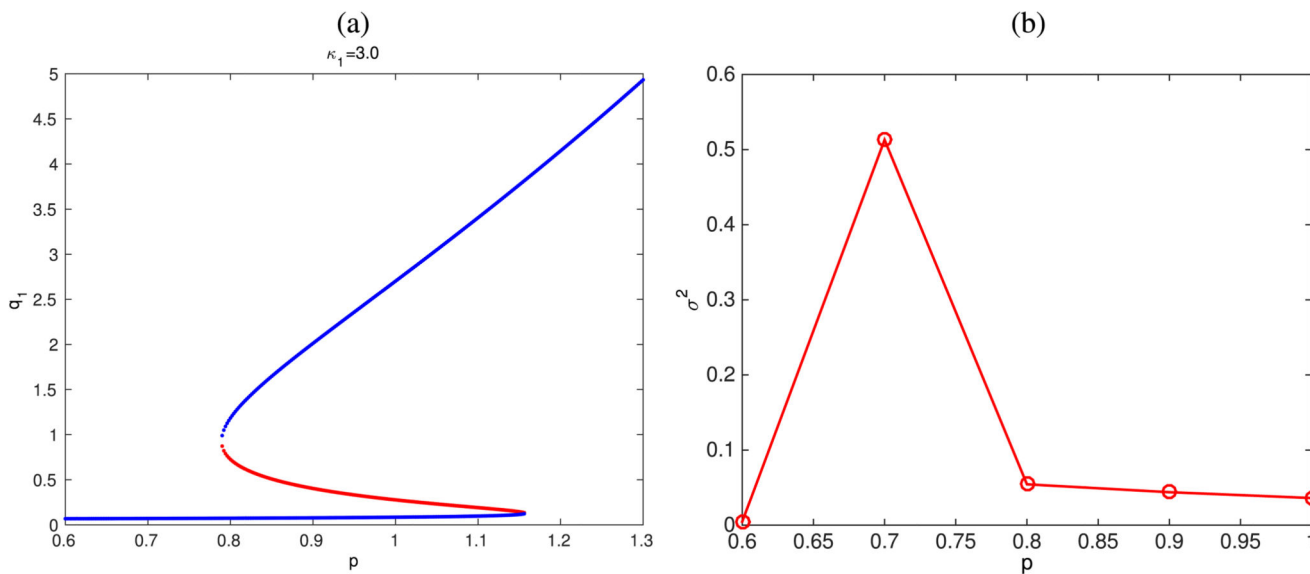
Fig. 9.

Plot (a): bifurcation analysis for the SCQSS approximation of the stochastic auto-activation gene regulatory circuit Eqs. (54) and (55), with $\kappa_1 = 3.0$. Parameter values as given in Table VI. Plot (b): simulation results for the variance $\sigma^2 = \langle (x_1 - \langle x_1 \rangle)^2 \rangle$, with $x_1 = X_1(\tau = T)/S$, associated to the simulation results shown in Fig. 8. This plot shows how σ^2 changes as the control parameter, p. The maximum of σ^2 as a function of the control parameter helps us to quantitatively determine the corresponding critical value.73

Table I

Random variables and transition rates of the stochastic model associated to the enzymatic reaction shown in Fig. 1.

Variable	Description
X_1, X_2	Number of active and inactive (respectively) Cdh1 molecules
X_3, X_4	Number of Cdh1-inactivating and Cdh1-activating (respectively) enzyme molecules
X_5, X_6	Number of enzyme-active Cdh1 and enzyme-inactive Cdh1 (respectively) complexes
X_7	Number of active cyclin molecules

Transition rate	r	Event
$W_1(x) = k_1 X_7 X_1 X_3$	$r_1 = (-1, 0, -1, 0, +1, 0, 0)$	Enzyme and active Cdh1 form complex
$W_2(x) = k_2 X_7 X_5$	$r_2 = (+1, 0, +1, 0, -1, 0, 0)$	Enzyme-active Cdh1 complex splits
$W_3(x) = k_3 X_7 X_5$	$r_3 = (0, +1, +1, 0, -1, 0, 0)$	Inactivation of Cdh1 and enzyme release
$W_4(x) = k_4 X_2 X_4$	$r_4 = (0, -1, 0, -1, 0, +1, 0)$	Enzyme and inactive Cdh1 form complex
$W_5(x) = k_5 X_6$	$r_5 = (0, +1, 0, +1, 0, -1, 0)$	Enzyme-inactive Cdh1 complex splits
$W_6(x) = k_6 X_6$	$r_6 = (+1, 0, 0, +1, 0, -1, 0)$	Activation of Cdh1 and enzyme release
$W_7(x) = k_7$	$r_7 = (0, 0, 0, 0, 0, 0, +1)$	CycB synthesis
$W_8(x) = k_8(1 + aX_1)X_7$	$r_8 = (0, 0, 0, 0, 0, 0, -1)$	CycB degradation

Table II

Dimensionless variables used in Eq. (29). S and E are the average concentration of Cdh1 (active plus inactive) and the average concentration of both Cdh1-activating and Cdh1-inactivating enzymes, respectively. We further assume that the stationary concentration of active CycB also scales with S.

Rescaled variables	Dimensionless parameters
$\tau = k_1 E S t$	$\epsilon = E/S,\ a = aS$
$q_1 = Q_1/S$	$\kappa_2 = k_2/(k_1 S)$
$q_2 = Q_2/S$	$\kappa_3 = k_3/(k_1 S)$
$q_3 = Q_3/E$	$\kappa_4 = k_4/(k_1 S)$
$q_4 = Q_4/E$	$\kappa_5 = k_5/(k_1 S^2)$
$q_5 = Q_5/E$	$\kappa_6 = k_6/(k_1 S^2)$
$q_6 = Q_6/E$	$\kappa_7 = k_7/(k_1 E S^2)$
$q_7 = Q_7/S$	$\kappa_8 = k_8/(k_1 E S)$

Table III

Parameter values used in simulations of the stochastic bistable enzyme-catalysed system.

Rescaled parameter	Parameter	Units	Reference
$\kappa_2 = J_4 - \kappa_3$	$a_1' = 0.04$	min^{-1}	22
$\kappa_3 m = \dfrac{a_4 m}{k_1 ES}$	$a_2' = 0.04$	min^{-1}	22
$\kappa_6 = \dfrac{a_3'}{k_1 ES}$	$a_2'' = 1$	min^{-1}	22
$\kappa_5 = \kappa_4 J_3 - \kappa_6$	$a_3 = 1$	min^{-1}	22
$\kappa_7 = \dfrac{a_1'}{k_1 ES}$	$a_4 = 35$	min^{-1}	22
$\kappa_8 = \dfrac{a_2'}{k_1 ES}$	$m = 0.3$	Dimensionless	…
$a = \dfrac{a_2''}{k_1 ES \kappa_8}$	$E = 0.01$	Dimensionless	38
	$S = 1.0$	Dimensionless	38
	$k_1 = 1$	min^{-1}	33
	$\kappa_4 = \kappa_3$	Dimensionless	38
	$J_3 = J_4 = 0.04$	Dimensionless	22

Table IV

Random variables and transition rates associated to the stochastic dynamics of an auto-activation gene regulatory circuit.[30,74] X_2 corresponds to the number of transcription-factor dimer/promoter binding site trimers. See Fig. 6 for a schematic representation.

Variable	Description
X_1	Number of transcription factor molecules
X_2	Number of bound promoter sites in the gene promoter region
X_3	Number of unoccupied (unbound) binding sites in the gene promoter region

Transition rate	r	Event
$W_1(x) = \hat{R} + k_1 X_2$	$r_1 = (1, 0, 0)$	Synthesis of the transcription factor
$W_2(x) = k_2 X_1$	$r_2 = (-1, 0, 0)$	Degradation of the transcription factor
$W_3(x) = k_3 X_1(X_1-1)X_3$	$r_3 = (-2, +1, -1)$	Dimer binding to the gene promoter region
$W_4(x) = k_4 X_2$	$r_4 = (+2, -1, +1)$	Unbinding from the gene promoter region

Table V

Dimensionless variables used in Eq. (29). s_0 is a characteristic scale associated to the average number of molecules of transcription factor, X_1, and E is the average number of binding sites in the promoter of the self-activating gene. We further assume that $S \gg E$.

Rescaled variables	Dimensionless parameters
$\tau = k_3 E S t$	$\epsilon = E/S, \ R = \hat{R}/(k_3 E S^2)$
$q_1 = Q_1/S$	$\kappa_1 = k_1/(k_3 S^2)$
$q_2 = Q_2/E$	$\kappa_2 = k_2/(k_3 E S)$
$q_3 = Q_3/E$	$\kappa_4 = k_4/(k_3 S^2)$

Table VI

Parameter values used in simulations of the stochastic self-activation gene regulatory circuit.

Rescaled parameter	Parameter	Units	Reference
$\kappa_1 = \dfrac{a}{k_{deg}\sqrt{K_d}}$	$K_d = 10$	nM	30
$\kappa_2 = 1$	$k_{\text{deg}} = 2$	min^{-1}	30
$\kappa_4 = 1$	$r = 0.4$	nM min^{-1}	30
$R = \dfrac{r}{k_{deg}\sqrt{K_d}}$	$S = 1.0$		…
$k_3 ES = k_{deg}$	$E = 0.1$		…